

Low endotoxin *E. coli* strain-derived plasmids reduce rAAV vector-mediated immune responses both *in vitro* and *in vivo*

Qingyun Zheng,¹ Tianyi Wang,¹ Xiangying Zhu,² Xiao Tian,¹ Chen Zhong,¹ Guolin Chang,³ Gai Ran,¹ Yilin Xie,¹ Bing Zhao,¹ Liqing Zhu,³ and Chen Ling¹

¹State Key Laboratory of Genetic Engineering and Engineering Research Center of Gene Technology (Ministry of Education), School of Life Sciences, Zhongshan Hospital, Fudan University, Shanghai 200438, China; ²Zhejiang Hengyu Biological Technology Co., Ltd., Jiaxing, Zhejiang Province 314113, China; ³Department of Clinical Laboratory, The First Affiliated Hospital of Wenzhou Medical University, Wenzhou, Zhejiang Province 325000, China

The major challenge of recombinant adeno-associated virus (rAAV) vectors is host immunological barriers. Compared to the neutralizing antibody and the cytotoxic T lymphocyte response, the host immune responses induced by unsatisfactory rAAV manufacturing were largely ignored previously. rAAV vector production usually requires large amounts of plasmid DNAs. The DNA are commonly isolated from the DH5 α bacterial strain, which contains lipopolysaccharide (LPS) contamination. LPS, also named endotoxin, in plasmid DNA is intractable, and residual endotoxin in the subsequent rAAV vectors may result in substantial host immune response. Recently, a ClearColi K12 bacterial strain is commercially available, with genetically modified LPS that does not trigger endotoxic response in mammalian cells. Here, we produced rAAV-DJ vectors by plasmids yielded from either DH5 α or ClearColi K12 bacterial strains. Our data indicated that the ClearColi K12 strain had satisfactory protection for the rAAV inverted terminal repeat (ITR) sequence. As expected, the ClearColi K12-derived rAAV-DJ vectors had lower endotoxin levels. The physical and biological equivalency of the purified viral stocks were confirmed by electron micrographs, Coomassie blue staining, and transduction assays. Most importantly, the ClearColi K12-derived rAAV-DJ vectors triggered reduced nuclear factor-kappa B (NF- κ B) signaling pathway both in cell cultures *in vitro* and in C57BL/6 mice retinas *in vivo*. We believe that the use of the ClearColi K12 bacterial strain could eliminate the LPS in the purified vector stock at the source. Our data indicate its promising use in future clinical development.

INTRODUCTION

Endotoxins, also called lipopolysaccharides (LPSs), consist of three parts: lipid A, core oligosaccharide, and O-antigenic polysaccharide side chain.¹ LPS exists in the outer membrane of gram-negative bacteria and is released after the death of bacterial cells.² In mammalian cells, Toll-like receptor 4 (TLR4) recognizes bacterial LPS, followed by activation of transcription factor nuclear factor-kappa B (NF- κ B) through myeloid differentiation primary response gene 88

(MyD88).^{3,4} Alternatively, LPS can induce NF- κ B by activating the Toll/interleukin (IL)-1 receptor domain containing adaptor-inducing IFN-beta (TRIF)-dependent pathway, which requires tumor necrosis factor- α (TNF α).⁵ NF- κ B is well-known to control the expression of an array of inflammatory cytokine genes, the first line of defense against invading pathogens.⁶ Most importantly, even a small amount as low as 10 endotoxin units (EU) can induce strong allergic reaction, septic shock, and death of a host organism. Therefore, therapeutics produced from *E. coli* bacteria must be extensively purified to remove endotoxin before administration.⁷

Recombinant adeno-associated virus (rAAV) vector is one of the leading platforms for *in vivo* delivery of gene therapeutics.⁸ They have shown great potential to treat a variety of human diseases, such as ocular, muscle, and liver diseases. Europe and the United States approved their first rAAV-based gene therapy product in 2012 and 2017, respectively. Currently, approximately 200 rAAV gene therapy clinical trials have been conducted worldwide. The beneficial features of rAAV vectors include non-pathogenicity, broad tropism, and long-term expression of transgenes.⁹ On the other hand, the limitations and challenges must be acknowledged, which include issues with rAAV manufacturing and host immunological barriers, such as cytotoxic T lymphocyte responses and neutralizing antibodies against rAAV capsid protein.¹⁰ However, the host immune responses induced by unsatisfactory rAAV manufacturing were largely ignored previously. rAAV vectors are often prepared by transfection of HEK293 cells with large amounts of plasmid DNA that was isolated from *E. coli*.¹¹ The current clinical acceptance criteria for endotoxin in the rAAV stocks is <2 EU/dose.¹² Purifying rAAV stocks to remove LPS will result in significant vector particle loss. Recently, a simple universal protocol was proposed to use mild detergent treatment.¹³

Received 1 March 2021; accepted 10 June 2021;
<https://doi.org/10.1016/j.omtm.2021.06.009>.

Correspondence: Chen Ling, PhD, State Key Laboratory of Genetic Engineering, School of Life Sciences, Zhongshan Hospital, Fudan University, 2005 Songhu Road, Shanghai 200438, China.

E-mail: lingchenchina@fudan.edu.cn



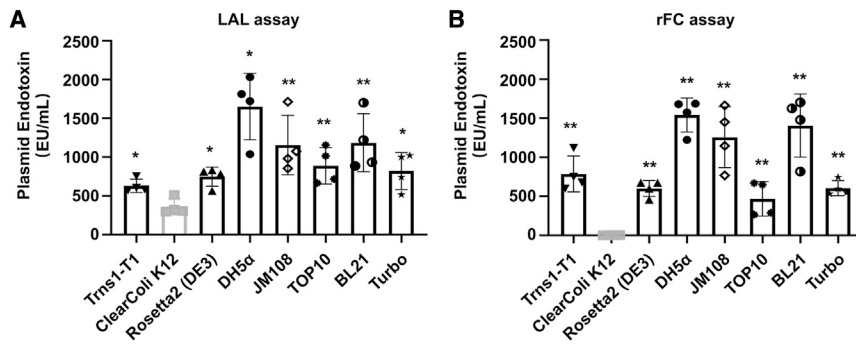


Figure 1. Plasmids derived from ClearColi K12 strain showed the lowest endotoxin level

The plasmids pAAV-*gfp* were prepared from indicated bacterial strains. The endotoxin levels were determined by either (A) *Limulus* ameobocyte lysate (LAL) assay, or (B) recombinant Factor C (rFC) assay. The measurements represented the means and standard deviations from four individual experiments. One-way ANOVA analysis with Tukey test. * $p < 0.05$ vs. ClearColi K12; ** $p < 0.01$ vs. ClearColi K12.

Thus, researchers usually purify plasmid DNA using commercial LPS-removing kits and silica-based ion-exchange resins. Unfortunately, LPS is a chemically stable molecule with a net-negative charge and is resistant to high pressures, extreme temperatures, and pH values.¹⁴

ClearColi K12 is a recently developed, genetically engineered *E. coli* strain for plasmid DNA preparation. The genetic modifications of LPS-related genes result in inability to cause an endotoxic response in human cells. Briefly, the polysaccharide chains and two secondary acyl chains of LPS have been deleted, by knocking out seven genes (Δ gutQ, Δ kdsD, Δ lpxL, Δ lpxM, Δ pagP, Δ lpxP, and Δ eptA). The resultant molecule, Lipid IVA, instead of LPS, is not recognized by TLR4 and consequently is ineffective in activating the NF- κ B pathway and producing pro-inflammatory cytokines. In this study, we compared the use of ClearColi K12 and DH5 α (a frequently used *E. coli* strain) during rAAV-DJ vector production. The physical and biological equivalency of the purified rAAV-DJ vector stocks were characterized, and their ability to activate the NF- κ B pathway was investigated both *in vitro* and *in vivo*. Our aim is to improve the safety of rAAV gene therapy products.

RESULTS

The electrocompetent ClearColi K12 cells generate rAAV plasmids with a lower endotoxin level

Limulus ameobocyte lysate (LAL) assay is traditionally used to assess endotoxin in samples. However, this assay is based on protease cascade and lacks specificity to discriminate between lipid A and lipid IVA, making it unsuitable for assessing rAAV-associated toxicity in this research. Thus, we decided to use recombinant Factor C (rFC) assay.¹⁵ The plasmid pAAV-*gfp* was isolated from various *E. coli* strains and subsequently tested for endotoxin contamination. In both LAL and rFC assays, 100 ng of plasmids from the ClearColi K12 strain showed the lowest endotoxin level, compared to those obtained from other commonly used rAAV plasmid-producing *E. coli* strains (Figure 1). As expected, the LAL assay gave a false positive with plasmids produced from the ClearColi strain. Then, electroporation-competent cells and chemically competent cells were made using either the ClearColi K12 strain or the DH5 α strain. In addition, a recently commercially available Mix & Go! *E. coli* Transformation Kit was used to prepare competent cells. As shown in Figure 2A, all

three methods could be applied for the DH5 α strain. However, for the ClearColi K12 strain, only the preparation of electrocompetent cells was successful. Then, we characterized the electrocompetent DH5 α and ClearColi K12 bacteria for their ability to transform 1 ng of plasmid pAAV-*gfp* and for their plasmid yields (Figure 2B). The number of colonies showed that the DH5 α -competent cells were three times more efficient than the ClearColi K12-competent cells. On the other hand, there was no reduction in plasmid yields, suggesting that the copy number of rAAV plasmids during the bacterial growth was not affected. As a key element flanking the AAV genome, the inverted terminal repeat (ITR) is unstable in *E. coli*. Thus, pAAV-*gfp* and pAAV-*fluc* plasmids were isolated from ten colonies of either DH5 α or ClearColi K12. The integrity of ITRs, which is indicated by the presence of SmaI sites, was confirmed by digestion with endonuclease. The digestion should give a plasmid backbone band corresponding to approximately 2.6 kb, plus bands that correspond to the size of the insert DNA between two ITRs (Figure 2C). The results of gel electrophoresis demonstrated that ClearColi K12 exhibited satisfactory protection for the ITR sequence (90% versus 100%; Figure 2D).

The ClearColi K12-derived plasmids have rAAV-DJ vector-producing ability similar to DH5 α -derived plasmids

Both DH5 α and ClearColi K12 bacteria were used to generate the plasmids required for triple transfection. Two genes of interest were selected, *gfp* and *firefly luciferase (fluc)* genes. As expected, all of the plasmid DNAs from ClearColi K12 had lower endotoxin content than DH5 α -derived counterparts, regardless of the detection methods (Figures 3A and 3B). Since the LAL assay gave false-positive results, the rFC assay was used in the subsequent experiments. To investigate the transfection ability, both DH5 α - and ClearColi K12-derived plasmids pAAV-*gfp* (Figure 3C) and pAAV-*fluc* (Figure 3D) were transfected into the rAAV-producing HEK293 cells. The transgene expression was determined 48 h post-transfection and showed no significant difference.

Next, both DH5 α - and ClearColi K12-derived plasmids were triple-transfected to generate the unpurified crude lysate of rAAV-DJ vectors, as described in the Materials and methods. Non-transfected HEK293 cells were used as a negative control. It was evident that ClearColi K12-derived rAAV-DJ vector crude lysate had lower

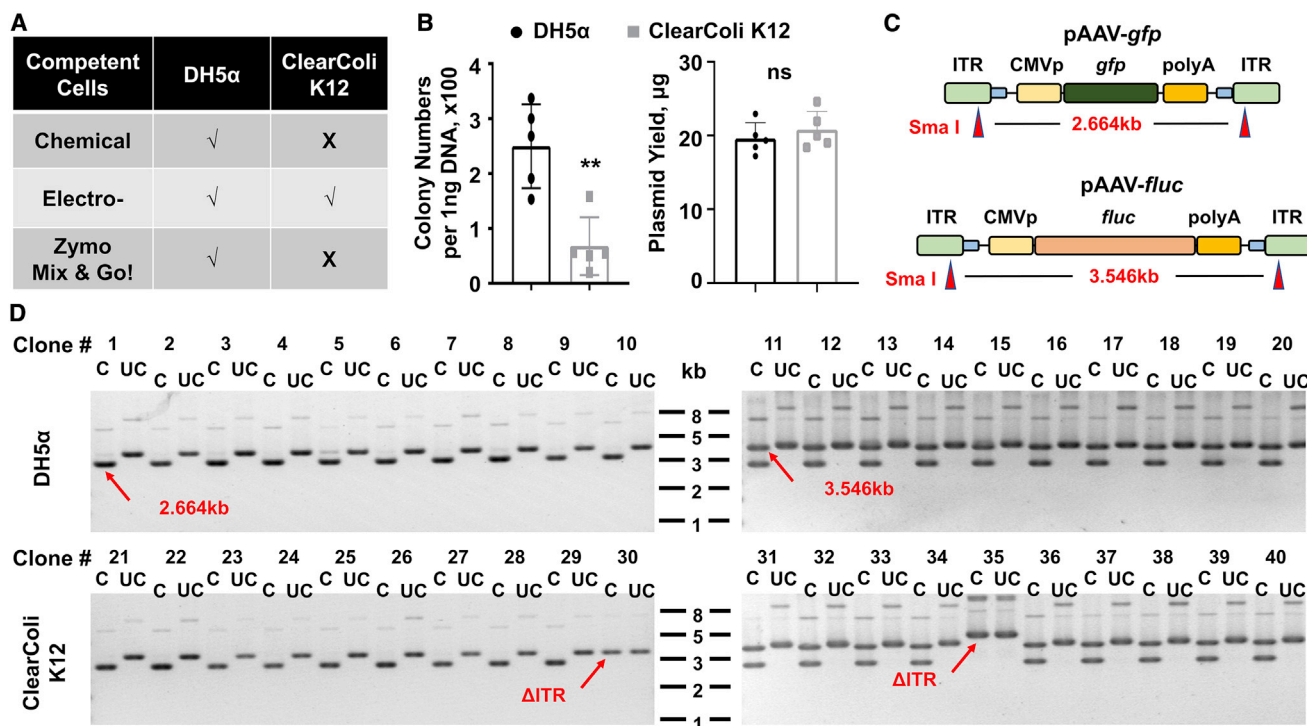


Figure 2. Electrocompetent ClearColi K12 had satisfactory protection for the rAAV ITR sequence

(A) Three methods could be applied to prepare competent DH5 α cells, while only electrocompetent ClearColi K12 cells were successfully generated for highly efficient DNA transformation. (B) Characterization of DH5 α - and ClearColi K12-derived colonies. Left: One nanogram of plasmid pAAV-*gfp* was transformed into electrocompetent ClearColi K12 and DH5 α bacteria. The number of colonies was counted. Right: Plasmid yields from electrocompetent DH5 α and ClearColi K12 cells. The measurements represented the means and standard deviations from five individual experiments. (C) Schematic diagrams of rAAV genome elements. Red triangle, SmaI site; ITR, inverted terminal repeat; CMVp, cytomegalovirus promoter; *gfp*, green fluorescence protein; *fluc*, firefly luciferase; polyA, polyadenylation signal. (D) Plasmids pAAV-*gfp* and pAAV-*fluc* were transformed into either DH5 α (upper) or ClearColi K12 (lower) electrocompetent cells. Plasmids from ten colonies of each group were isolated, digested by SmaI. The results of gel electrophoresis are shown. Red arrows with number, corrected plasmids with two ITRs; red arrows with Δ ITR, truncated plasmids with one ITR; C, SmaI cut; UC, uncut control. ** $p < 0.01$ vs. DH5 α .

endotoxin contents than DH5 α -derived counterparts (Figure 4A). Meanwhile, the titers of produced viral vector indicated that DH5 α - and ClearColi K12-derived plasmids had similar rAAV-generating ability (Figure 4B). Furthermore, the crude lysate was used to transduce HEK293 cells. The results showed similar transgene expression 48 h post-transduction, confirming that similar titers of rAAV-DJ vectors were produced by two kinds of plasmids (Figure 4C). In addition, the DH5 α -derived plasmids were prepared by QIAGEN Endofree Plasmid Maxi Kit, followed by producing unpurified rAAV crude lysate. Although lower endotoxin was observed in the DH5 α /QIAGEN-derived plasmids, there was no significant difference between the DH5 α /QIAGEN- and ClearColi K12/Axygen-derived vector crude lysates (Figure 4D). There was no significant difference in the transduction efficiency (Figure 4E).

The ClearColi K12-derived, purified rAAV-DJ vector stocks have reduced ability to activate NF- κ B pathway *in vitro*

Both DH5 α - and ClearColi K12-derived rAAV-DJ vectors were purified as indicated in the Materials and methods. It was evident that the ClearColi K12-derived rAAV-DJ vector stocks had a 5-time lower

endotoxin level compared to their DH5 α -derived counterparts (Figure 5A). SDS-PAGE analysis followed by Coomassie blue staining of vector preparations showed that all inter-lots of rAAV-DJ vectors had similar purity, ranging from 91.9% to 94.9%, as determined by optical density scanning of the gels (Figure 5B). The ratio of empty versus full particles was determined by negative staining with uranyl acetate using transmission electron microscopy (TEM), showing a comparable level for both vectors with no detectable particle aggregates (Figure 5C). To evaluate the transduction efficiency, both purified vectors were used to transduce HEK293, THP-1 (human acute monocytic leukemia), RAW264.7 (mouse macrophage), ARPE-19 (human retinal pigment epithelia), and Neuro-2a (mouse neuroblast) cells *in vitro*. Flow cytometry analysis revealed no significant difference between the two vector stocks (Figure 5D). The transgene expression in the adherent HEK293 cells was also analyzed by fluorescent microscopy, the results of which again indicated no difference in the transduction efficiency (Figures S1A and S1B). In addition, the transduction efficiency of ClearColi K12-derived rAAV-DJ vector was significantly higher than that of ClearColi K12-derived rAAV2 vector (Figure S1C), which is consistent with the previous reports.¹⁶

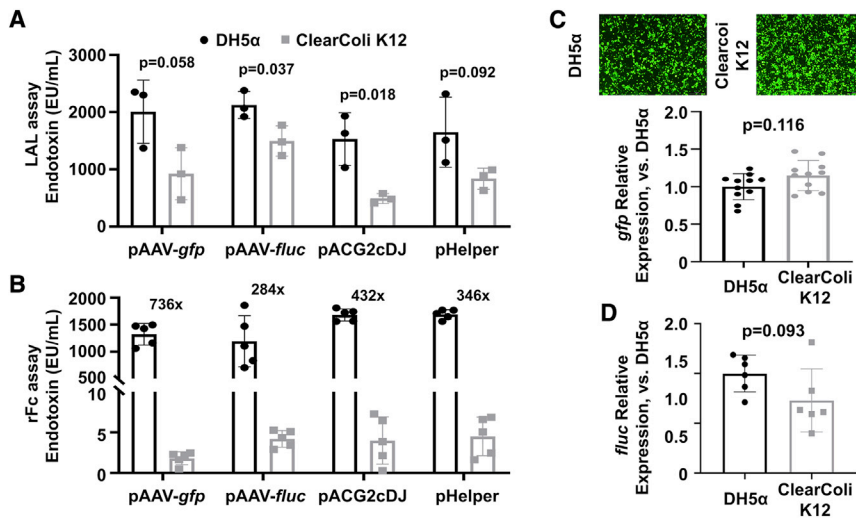


Figure 3. ClearColi K12-derived plasmids had sufficient transfection efficiency

Plasmids pAAV-DJ, pAAV-helper, pAAV-gfp, and pAAV-fluc were isolated from either the ClearColi K12 or DH5 α bacteria cells. Both (A) LAL assay, and (B) rFc assay showed that plasmids derived from ClearColi K12 had lower endotoxin levels. $n = 3$ for LAL assay; $n = 5$ for rFc assay. Plasmids (C) pAAV-gfp, and (D) pAAV-fluc were transfected into HEK293 cells, from which the transfection efficiency was determined 48 h post-transfection, by fluorescent microscope and luciferase assay, respectively. $n = 11$ for pAAV-gfp; $n = 6$ for pAAV-fluc. One-way ANOVA analysis with Tukey test.

A critical event downstream of LPS stimulation is the NF- κ B- and interferon regulatory factor (IRF)-dependent transcriptional activation of various inflammatory mediators, such as TNF α . In addition, the TLR4-MD2-CD14 complex that specifically recognizes the lipid A structure of LPS¹⁷ is potently upregulated by LPS.¹⁸ Thus, a mouse macrophage cell line, RAW264.7,¹⁹ was transduced with both vectors to investigate the rAAV-DJ vector-induced inflammatory responses *in vitro*. It was evident that the cells transduced with the DH5 α -derived rAAV-DJ vectors grew more slowly than those transduced with the ClearColi K12-derived rAAV-DJ vectors (Figure S2). Most importantly, the intracellular expression of IL-1 β at both the mRNA level (Figure 6A) and the protein level (Figure 6B) were significantly induced upon LPS treatment at 1 EU/mL and upon transduction with DH5 α -derived rAAV-DJ vectors. Meanwhile, transduction with ClearColi K12-derived rAAV-DJ vectors had little induction of IL-1 β expression, which was also confirmed by ELISA assays to determine the secreted protein in the cell culture medium (Figure 6C). In addition to the IL-1 β , other components of the NF- κ B pathway were also significantly overexpressed upon transduction with the DH5 α -derived rAAV-DJ vectors but not transduction with the ClearColi K12-derived rAAV-DJ vectors (Figure 6D). Similar results were obtained from a human monocytic cell line, THP-1 (Figure S3), which was commonly used for inflammatory properties in LPS-stimulated studies.²⁰

The ClearColi K12-derived, purified rAAV-DJ vector stocks induce lower ocular microglia activation and inflammatory cytokine expression

Despite the concept of ocular immune privilege, evident inflammation in treated eyes was reported in both non-human primates and clinical gene therapy trials.²¹ Thus, we would like to analyze the short-term ocular innate immune responses against the endotoxin and its potential long-term effect on the transgene expression. The purified rAAV-DJ viral vectors expressing a *gfp* gene under the control of a cytomegalovirus (CMV) promoter were injected subretinally

into the C57BL/6 mice. No difference was observed between mock-injected mice and rAAV-DJ vector-injected mice, in term of conjunctival congestion, secretion, and corneal edema. At 2 days post-injection, the retinas were harvested for histological analysis of microglia, which are the main innate immune cell type in the retina, and for detection of proinflammatory cytokine expression, while another group of mice was kept for determining the vector-mediated transgene at 60 days post-injection (Figure 7A). Iba1, a marker of microglia, was examined by immunofluorescent staining. There were significantly more Iba1-positive microglia in the outer nuclear layer (ONL) and subretinal space of retina after infection with the DH5 α -derived rAAV-DJ vectors (Figure 7B). We also evaluated the expression of proinflammatory cytokines at the mRNA level in the dissected retinas at 2 days post-injection. IL-6, TNF- α , and IL-1 β were highly upregulated in retinas transduced with DH5 α -derived rAAV-DJ vectors but not in those transduced with ClearColi K12-derived rAAV-DJ vectors (Figure 7C). For the long-term group of mice, no difference was observed between the mice injected with K12- or DH5 α -derived rAAV-DJ vectors in terms of conjunctival congestion, secretion, and corneal edema. It was evident that both vectors possessed comparable robust transgene expression in cone photoreceptors and the retinal pigment epithelium (RPE) (Figure 7D; Figure S4A). Meanwhile, the remaining rAAV-DJ vector genome copy numbers are comparable (Figure S4B).

DISCUSSION

rAAV is the vector of choice for ocular diseases. The US Food and Drug Administration (FDA) requires that intraocularly delivered gene therapy drugs should not exceed 2.0 EU/dose/eye or not more than 0.5 EU/mL of endotoxin. LPS is accompanied by the release of inflammatory cytokines such as IL-1 β , which will finally trigger pyroptosis.²² The lipid A structure of LPS is recognized by the membrane-bound TLR4-MD2 complex,¹⁷ which enables the innate immune system to monitor for bacteria agents. The signal was transduced via the adapter MyD88/TRIF to activate NF- κ B-mediated transcription of cytokines and chemokines. LPS-induced excessive TLR4 activation and the consequent cytokine storm may lead to endotoxic shock or sepsis.²³ On the other hand, the TLR4 pathway is not activated by rAAV transduction if the vector stocks contained

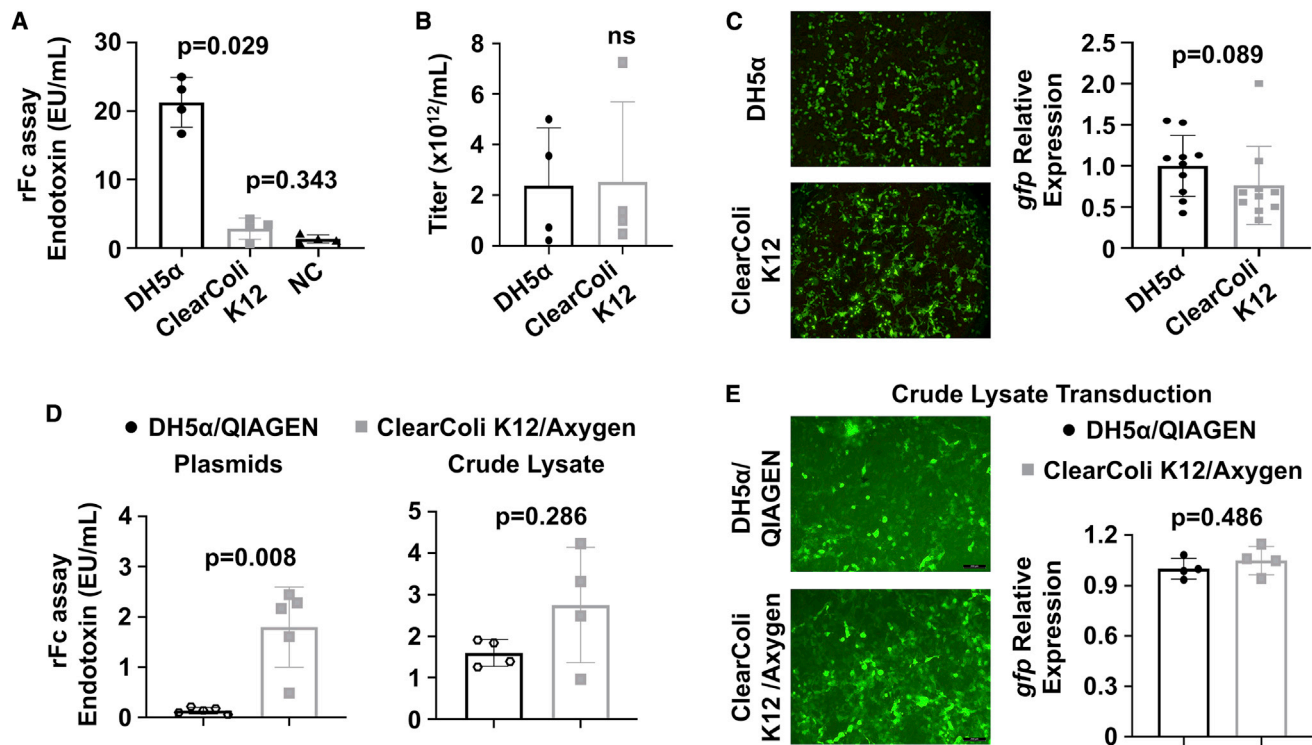


Figure 4. ClearColi K12-derived rAAV-DJ vector crude lysate had sufficient transduction efficiency

(A–C) rAAV-DJ vector crude lysate was prepared from DH5α- or ClearColi K12-derived plasmids. (A) The endotoxin levels, and (B) the titers of rAAV-DJ vector crude lysate were determined by rFc assay and qPCR assay, respectively. (C) HEK293 cells were transduced with rAAV-DJ vector crude lysate at MOI of 10E4 vg/cell. The transgene expression was determined by fluorescent microscopy 48 h post-transduction. (D and E) rAAV plasmids were isolated from ClearColi K12 bacteria cells by a regular Axygen kit. Alternatively, they were isolated from DH5α bacteria cells by a QIAGEN Endofree kit. rAAV-DJ vector crude lysate was prepared from those plasmids. (D) The endotoxin levels of rAAV plasmids (left) and rAAV-DJ vector crude lysate (right) were determined by rFc assay. (E) HEK293 cells were transduced with rAAV-DJ vector crude lysate at MOI of 10E4 vg/cell. The transgene expression was determined by fluorescent microscopy 48 h post-transduction. The measurements represented the means and standard deviations from at least four individual experiments. One-way ANOVA analysis with Tukey test.

less than 0.005 EU of endotoxin/mL.²⁴ There are two main sources of endotoxin contamination for rAAV viral stock: bacterial endotoxin and environmental endotoxin. It was proposed that the chemical nature of LPS allows intricate micelle structures to interact with viral particles. The commonly used method of affinity chromatography for LPS removal is time consuming, expensive, and usually fails, resulting in poor vector recoveries. Thus, it is important to eliminate the endotoxin at the source.

ClearColi technology produces a modified LPS, named Lipid IVA, that does not trigger the endotoxic response in human cells. Another ClearColi strain, BL21(DE3), has been increasingly used in the production of proteins,^{25–27} as well as virus-like particles for vaccines.²⁸ To our knowledge, this is the first time that the ClearColi technology has been used to produce low-endotoxin rAAV vectors. We observed that the ClearColi K12 strain has small colonies for the first 24 h after plating transformants. Although it grew more slowly than DH5α cells in liquid medium, plasmid yields from the ClearColi K12 cells were equal when grown to sufficient densities. Critical to the rAAV vector production, the ClearColi K12 cells have a genotype of ΔrecA. RecA is

a recombinase responsible for recombination between homologous DNA. It tends to knock out the ITR regions of rAAV genomes. Indeed, both ClearColi K12 and DH5α have similar protection effect on the ITR regions (Figure 2D). Moreover, both DH5α and ClearColi K12 are endA deficient, while another commonly used Stb3 line is endA+, which requires an additional wash step for column-based DNA preparation and consequently was not evaluated in this study.

LAL assay is traditionally used to assess endotoxin in samples. However, reactivity in the LAL assay requires the 4'-monophosphoryl-di-glucosamine backbone structure, which is present in both hexa-acylated LPS and tetra-acylated lipid IVA of *E. coli*. Thus, false-positive results occur that are due to the lack of specificity of the assay.²⁹ On the other hand, the Lucigen manual recommends a Recombinant Factor C Endpoint Fluorescent Assay to detect ClearColi-derived plasmids, which was used in this study. Being the initial component of the clotting cascade, rFC exhibits exceptionally high affinity for lipid A, which is not dependent on the activation of the protease cascade.³⁰ In the rFC test, the binding of endotoxin activates the synthetic rFC molecule, followed by cleavage of a fluorogenic substrate to

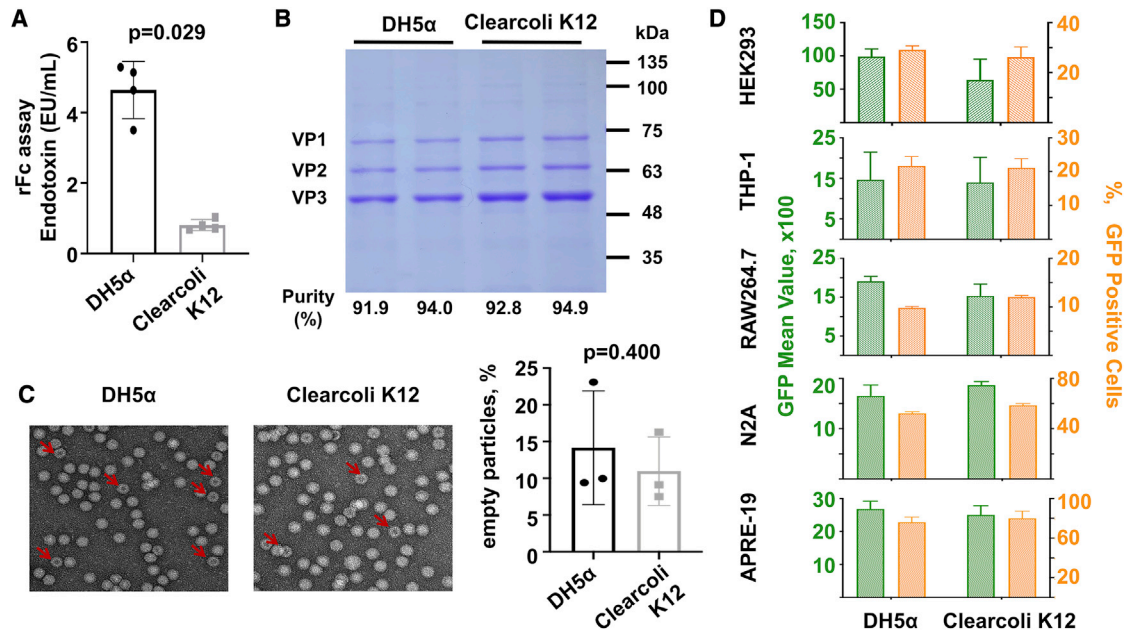


Figure 5. ClearColi K12-derived purified rAAV-DJ vectors had sufficient transduction efficiency

(A–D) Purified rAAV-DJ-*gfp* vectors were prepared from DH5 α - or ClearColi K12-derived plasmids. (A) The endotoxin levels were determined by rFC assay. $n = 4$. (B) Coomassie blue staining was performed after loading 5×10^{11} viral genomes per lane. Purity (% of VP1, VP2, and VP3 within total proteins) is indicated below gel image for each inter-lot vector. (C) Representative images of electron micrographs from each production group are shown. Empty particles (red arrow) were identified if the center of the capsid showed an electron-dense circle. The number of empty and full rAAV-DJ particles was counted from five images of electron micrographs. The average percentage of empty particles was quantified for each sample preparation. $n = 3$. (D) HEK293, THP-1, RAW264.7, Neuro-2a (N2A), and ARPE-19 cells were transduced with the purified rAAV-DJ vectors at MOI of $10E4$ vg/cell. The transgene expression was determined by flow cytometry 48 h post-transduction. The measurements represented the means and standard deviations from at least four individual experiments.

generate a fluorogenic compound.³¹ Recently, genetic engineering approaches based on modification of Factor C were developed for endotoxin quantification.³² Their advantages in the case of evaluating the products from ClearColi K12 cells require further exploration. Nevertheless, the most convincing endotoxicity test is the activation of immune responses in human cells *in vitro* and in animals *in vivo*. Our data suggested that ClearColi-derived vectors can safely and effectively downregulate innate immune responses without compromising transgene expression both *in vitro* and *in vivo*. This is presumably because the innate immune responses are neither vector capsid nor transgene specific. However, the long-term effects on the histopathological changes require further investigation.

The major limitation of using the ClearColi K12 bacterial strain is that its electro-transformation efficiency is lower than commonly used DH5 α . The efficiency is affordable for single-plasmid transformation, in which one or two colonies are enough. However, it is not acceptable to prepare large plasmid libraries of rAAV capsid mutants for directed evolution.³³ During directed evolution, it is desirable to transform each single DNA into the competent bacteria. This step requires the transformation efficiency to be as high as possible. In conclusion, we described here that isolating plasmid DNA from low endotoxin *E. coli* strain is a simple strategy to reduce the endotoxin level in rAAV preparations. Importantly, this method can be applied

for not only academic laboratories but also large-scale vector production for clinical developments.

MATERIALS AND METHODS

Bacteria

The genotypes of ClearColi K12 and DH5 α were F- λ - Δ *enda* Δ *recA* *frl181* *msbA52* Δ *gutQ* Δ *kdsD* Δ *lpxL* Δ *lpxM* Δ *pagP* Δ *lpxP* Δ *eptA* and F- ϕ 80 *lac* Δ M15 Δ (*lacZYA-arg F*) U169 *endA1* *recA1* *hsdR17*(*rk-mk+*) *supE44* λ -*thi-1* *gyrA96* *relA1* *phoA*, respectively.

Making chemically competent cells and transformation of plasmids

Ten milliliters of starter culture was inoculated into 1 L of lysogeny broth (LB) media. The optical density 600 (OD₆₀₀) was measured every hour, until the value was 0.4. The bacterial sample was centrifuged at 3,000 rpm for 20 min and resuspend in 5 mL ice-cold 100 mM CaCl₂. The bacterial sample was again centrifuged, and each pellet was resuspended in 0.5 mL ice-cold 100 mM CaCl₂, without vortexing. The bacterial sample was aliquoted into single-use Eppendorf tubes, 50 μ L for each tube. One nanogram of plasmid was added into each tube and incubated on ice for 30 min, followed by heat shock at 42°C for 30 s, then chilled again on ice for 5 min. The bacterial sample was outgrown in 1 mL LB for 1 h at 37°C and plated on selective plates.

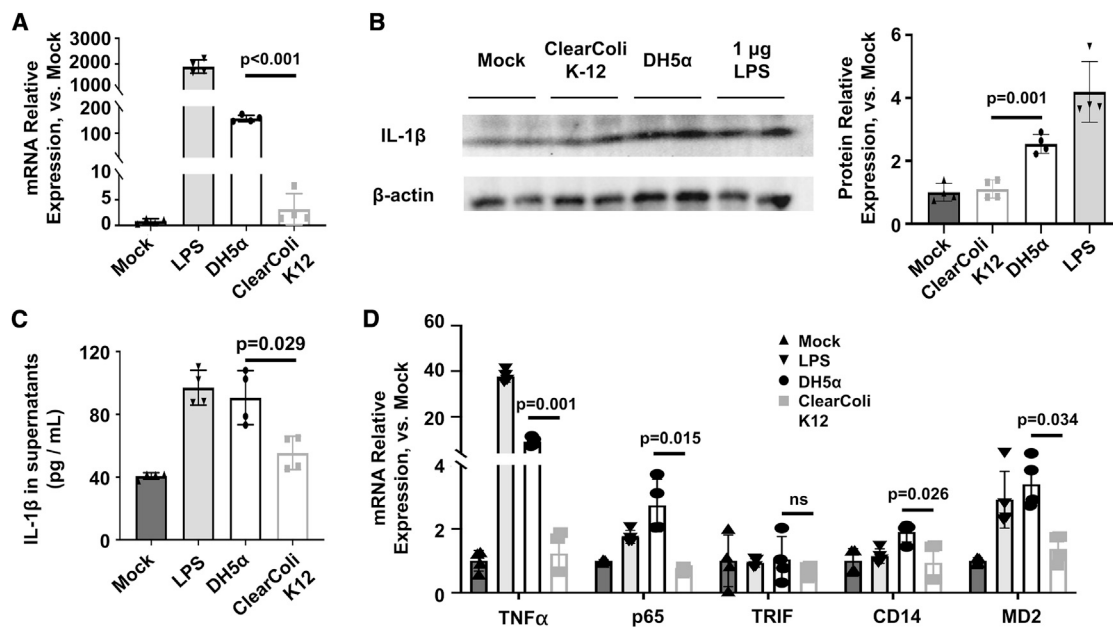


Figure 6. ClearColi K12-derived purified rAAV-DJ vectors induced lower inflammatory responses

RAW264.7 cells were transduced with DH5α- or ClearColi K12-derived purified rAAV-DJ-*gfp* vectors for 48 h. Alternatively, the cells were challenged with 1 μg/mL LPS as positive controls. (A and B) The expression of IL-1β was determined at the (A) mRNA level, and (B) protein level by quantitative real-time PCR and western blot assays, respectively. Expression level was normalized to β-actin. (C) The release of IL-1β in supernatants was analyzed by ELISA assay. (D) The expression of NF-κB pathway genes at the mRNA level was determined by quantitative real-time PCR. Expression level was normalized to β-actin. The measurements represented the means and standard deviations from four individual experiments. One-way ANOVA analysis with Tukey test.

Making electrocompetent cells and transformation of plasmids

Ten milliliters of starter culture was inoculated into 1 L of LB media. The OD₆₀₀ was measured every hour, until the value was 0.4. The bacterial sample was immediately chilled on ice for 30 min, along with other materials such as centrifuge bottles. The bacterial sample was centrifuged and resuspended for three rounds, ending with resuspension in 10 mL of ice-cold deionized H₂O. The bacterial sample was then centrifuged at 3,000 rpm for 20 min and resuspended in 1 mL of ice-cold 10% glycerol by gently swirling. The bacterial sample was aliquoted into single-use Eppendorf tubes, 50 μL for each tube. One nanogram of plasmid was added into each tube, followed by vortexing and transferring into a precooled 0.1-cm-gap sterile electroporation cuvette. The sample was kept on ice for 10 min. Then, it was subjected to electric shock at the voltage of 1.8 kV, followed by adding 1 mL recovery medium (Weidi Biotechnology, Shanghai, China) immediately. The sample was shaken at 37°C, 230 rpm for 40 min, from which 100 μL was taken to coat the ampicillin plate. The mono-colonies of ClearColi K12 and DH5α can be picked up after 24 h and 16 h, respectively.

Making Zymo Mix & Go!-competent cells and transformation of plasmids

Mix & Go! *E. coli* Transformation Kit was purchased from Zymo Research (cat. no. T3001, Irvine, CA, USA). The competent cells were made, and transformation of plasmids was performed according to the manufacturer's guidelines.

Cell culture

The human embryonic kidney (HEK)293, THP-1, RAW264.7, ARPE-19, and mouse N2A cells were obtained from the American Type Culture Collection (Manassas, VA, USA). HEK293, RAW264.7 cells were cultured in complete Dulbecco's modified Eagle's medium (C-DMEM) replenished with 10% fetal bovine serum (FBS) and 1% penicillin-streptomycin, THP-1 cells in complete Roswell Park Memorial Institute (RPMI)-1640 medium, ARPE-19 cells in ATCC-formulated DMEM:F12 medium, and N2A cells in ATCC-formulated Eagle's minimum essential medium. All cells were grown in a cell incubator at 37°C in an atmosphere containing 5% CO₂.

Plasmid isolation

Plasmid DNAs were isolated using the alkaline-based Axygen Axy-Prep Plasmid Miniprep and Maxiprep Kit (Corning, Wujiang, Jiangsu, China) according to the manufacturer's guidelines. Briefly, the bacterial samples were resuspended in 200 μL of ice-cold resuspension Buffer S1, followed by treatment with 200 μL of lysis Buffer S2 containing NaOH and SDS for 4 min. The samples were neutralized with 200 μL of chilled Buffer S3 and centrifuged at 8,000 × g for 10 min at 4°C. The supernatant containing the plasmid was further purified using a special column. The DNAs were finally eluted by deionized water. The plasmid DNA was quantified by a Nanodrop Lite, according to the manufacturer's instructions. Each plasmid sample was measured 3 times to make an average of quantity. The ratio of 260/280 was used as an indicator of the purity. A purity range from

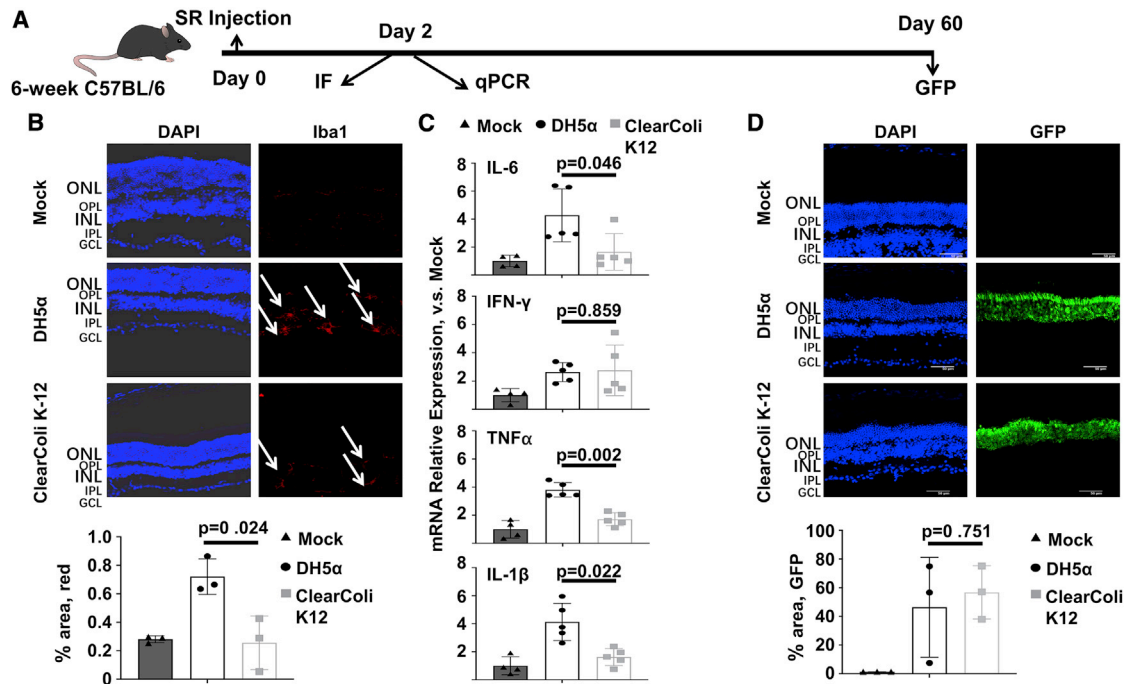


Figure 7. ClearColi K12-derived purified rAAV-DJ vectors induced lower activation of microglia and innate immune response

(A) Schematic of the *in vivo* experimental design. Mouse eyes were subretinally injected with rAAV-DJ-*gfp* vectors (1×10^{10} vg/eye). (B and C) The retinas were collected 2 days post-injection for (B) immunofluorescent staining against Iba1, and (C) relative mRNA levels of IL-6, IFN- γ , TNF- α , and IL-1 β by qPCR assays. Quantification of displaced Iba1-positive area (white arrow) by ImageJ. Expression levels of mRNA were normalized to β -actin. (D) The retinas were collected 60 days post-injection for detection of transgene expression. Exemplar images of transverse sections through mouse retinas. Quantification of displaced GFP-positive area by ImageJ. The measurements represented the means and standard deviations from three to five mice eyes. One-way ANOVA analysis with Tukey test.

1.80 to 2.00 was considered as acceptable. To further corroborate the results, each plasmid sample was confirmed by enzymatic digestion, followed by gel electrophoresis.

PEI-mediated plasmid transfection

The linear polyethylenimine (PEI) hydrochloride (molecular weight [MW] 40,000) was purchased from Polysciences (23966-1, Warrington, PA, USA). The PEI was weighed and dissolved in deionized water to prepare 1 mg/mL stock, sterilized with 0.2 μ m filter, aliquoted, and kept at -80°C . For each 15 cm plate with healthy 80% confluent cells, the following transfection solution was prepared: 950 μ L DMEM without serum or antibiotics, 60 μ g plasmid DNA, and 125 μ L PEI. The transfection solution was incubated for 10 min at room temperature and drop-wise added into the plate, while gently swirling it. The plate with cells was incubated at 37°C , 5% CO_2 for 6 h, followed by replacing media with complete media.

rAAV-DJ vector production

PEI-mediated triple-plasmid (gene of interest, rAAV-DJ capsid protein plasmid and pAAV-helper) transfection method was used to produce rAAV vectors, as previously described.³⁴ Briefly, HEK293 cells were harvested 72 h post-transfection. The cell pellet was resuspended in 5 mL of RB TMS Buffer (50 mM Tris-HCl, 150 mM NaCl [pH 8.0]), followed by three repeats of freeze in dry-ice-ethanol bath for

10 min and thaw at 37°C for 10 min, to prepare the crude lysate. The lysate was spin down at 3,000 rpm, 4°C for 10 min, and the supernatant was collected for Benzonase digestion (EMD Millipore, Darmstadt, Germany). In a 13 mL Quick-Seal centrifuge tube (Beckman Coulter, 342413, Brea, CA, USA), the supernatant was loaded on top of iodixanol gradient (OptiPrep, cat. no. 1114542, Sigma-Aldrich Inc., St. Louis, MO, USA). The samples were ultra-centrifuged at 75,000 rpm for 1 h, and the 40% iodixanol fraction was collected. Finally, the vectors were further purified by ion exchange chromatography using HiTrap Q column (GE Healthcare, Piscataway, NJ, USA), washed with phosphate-buffered saline, and concentrated using centrifugal spin concentrators with 150 K molecular-weight cutoff. Viral vectors were finally resuspended in 500 μ L PBS.

Determination of rAAV vector titer

All vector preparations were subjected to quantitative real-time polymerase chain reaction (PCR) to test the virus titer. Briefly, 10 μ L of vector stock was digested with Benzonase (EMD Millipore, Darmstadt, Germany) at 37°C for 1 h. Then, NaOH and SDS were added to make the final concentration at 100 mM and 0.2%, respectively. The samples were incubated at 65°C for 30 min. A series of plasmid DNAs with known quantity were denatured in the same manner for the use as a reference standard for quantitation. No template water control was also used in each run. The vector DNAs were purified

by DNA Clean & Concentrator-25 Kit (Zymo Research, Irvine, CA, USA) and subjected to qPCR assays. Reaction mixtures in a final volume of 20 μL consisted of 10 μL of Fast qPCR Mix based on SYBR Green I (TsingKe Biotech, Beijing, China), 0.5 μL of primers at 1 μM , and 9.5 μL of AAV template with deionized water. The ITR primers F: 5'-GGAACCCCTAGTGATGGAGTT-3' and R: 5'-CGGCCTCAGTGAGCGA-3' were used. Forty cycles of three-step thermal profile were performed, composed of 10 s at 95°C, 5 s at 55°C, and 10 s at 72°C.

rAAV-DJ vector transduction *in vitro*

Briefly, suspension cultures of THP-1 and RAW264.7 cells were seeded in 96-well (1×10^5 cells) or 6-well (2×10^6 cells) plates in FBS- and antibiotic-free medium. LPS or rAAV vectors (2,000 vg/cell) were added at the time of seeding. Cells were spanned down 4 h post-transduction, followed by replacement of FBS- and antibiotic-free medium with C-DMEM. Cells were then harvested and washed by PBS twice at 72 h post-transduction and analyzed by Calibur Flow Cytometer (BD Biosciences, San Jose, CA, USA), using the 488 nm excitation laser and 530–540 nm emission filter to measure the EGFP fluorescence. Alternatively, quantitative real-time PCR and Western blot assays were performed to measure inflammation-related gene expression at 16 h post-transduction.

LPS detection

The plasmids were diluted to 10 ng/mL and the viral stocks to $10E10$ vg/mL in endotoxin-free water. LPS levels were determined by LAL assay (Thermo Scientific, cat. no. A39552S) and Rhinolyse Recombinant Factor C Endpoint Fluorescent Assay (RAF-01, Suzhou RhinoBio, Suzhou, China), according to the supplier's instructions. The linear range was roughly between 0.1 and 20 EU/mL.

Quantitative reverse-transcription polymerase chain reaction (RT-PCR)

Total RNAs were collected by the RNA extracting kit (cat. no. 9767, Takara Bio, Shiga, Japan). Template complementary DNA (cDNA) was reverse transcribed by oligo-d(T) or random 6 mer primers (RR036A, Takara Bio, Shiga, Japan). RT-PCR analysis was carried out in triplicates using $2 \times T5$ SYBR Green Fast qPCR Mix (TSE202, Tsingke Biological Technology, Beijing, China) and cDNA samples from independent RNA sets. All primers used for qPCR reactions are listed in Table S1. Standard amplification conditions were used, which consisted of thirty cycles of denaturation at 94°C for 30 s, annealing at 55°C for 30 s, and extension at 72°C for 30 s. The relative amount of target mRNA was calculated using the $\Delta\Delta\text{CT}$ method and normalized against reference gene (β -actin) in each sample.

Western blot analysis

Western blot assays were performed as previously described.³⁵ Briefly, cells were harvested after the indicated treatment, rinsed by PBS, and disrupted in lysis buffer (P0013B, Beyotime Biotechnology, Shanghai, China). The total protein was determined and normalized by BCA Protein Assay Kit (P0012, Beyotime Biotechnology,

Shanghai, China). Samples were separated by 10% SDS-PAGE electrophoresis, electro-transferred to a poly-vinylidene difluoride transfer (PVDF) membrane, and probed with relevant primary antibodies at 4°C overnight (anti-IL-1 β [1:1,000, B122, Santa Cruz, Santa Cruz, CA, USA] or anti-actin primary antibody [1:3,000, AF0006, Beyotime Biotechnology, Shanghai, China]). The membranes were then incubated with horseradish peroxidase-conjugated secondary antibody (1:5,000, A0208, Beyotime Biotechnology, Shanghai, China) and detected with an enhanced chemiluminescence substrate (Tanon, Shanghai, China).

Cell viability assay

Cell viability was detected by the Cell Counting Kit-8 (CCK-8, Dojindo Molecular Technologies, Gaithersburg, MD, USA) according to the instructions.³⁶ Cells were seeded in 96-well plates at 10,000 cells per well in C-DMEM, followed by transduction with rAAV-DJ vectors. CCK-8 solution was added to each well as the manufactory protocol suggests. Plates were incubated for 4 h at the same incubator conditions, after which the absorbance was read at 450 nm using a VERSAmix tunable microplate reader (Sunnyvale, CA, USA).

Animals

Animal experiments were operated at School of Life Sciences, Fudan University, Shanghai, China, under the Institutional Animal Care and Use Committee approval, #2020JS-027. Eight-week-old male C57BL/6 mice (Charles River, Beijing, China) were bred and maintained in the animal facility of Fudan University. All animal procedures were performed in line with the ARVO Statement for the Use of Animals in Ophthalmic and Vision Research. Mice were divided into three groups and performed the subretinal injections. The limbus cornea was pierced with insulin disposable needle and a 34-gauge blunt-tip needle was introduced into the subretinal space. Each eye received 1 μL of vector at a titer of 1×10^{13} vg/mL, or corresponded volume of PBS as untreated control. The mice were euthanized and the eyeballs were removed after 1 month post injection for subsequent studies. Fluorescent images were obtained by confocal microscope (FV3000, Olympus, Shinjuku, Tokyo, Japan).

TEM for viral vectors

Ten microliters of purified rAAV-DJ vectors ($10E11$ vg/ μL) was placed on a freshly glow-discharged formvar-carbon-coated 230 mesh copper grid for 5 min. Excess liquid was drained off by filter paper. The grid was stained with 5 μL 3% uranyl acetate for an additional 5 min and was examined by a Thermo Scientific Talos L120C TEM with the acceleration voltage of 120 kV. The TEM pictures of the rAAV-DJ particle were measured and analyzed for length of the minor and major axes using the IMS cell image analysis system.

Statistical analysis

The GraphPad Prism 8.2.1 (GraphPad, San Diego, CA, USA) was used to process statistical analyses. The nonparametric Mann-Whitney U test was used to analyze the discrepancies between two sets. Two-group comparison used the one-way ANOVA, and

$p < 0.05$ was considered significantly different. All experimental results were operated at least in triplicate.

SUPPLEMENTAL INFORMATION

Supplemental information can be found online at <https://doi.org/10.1016/j.omtm.2021.06.009>.

ACKNOWLEDGMENTS

The authors thank Mrs. Chunbao Sun at the University of Florida, Gainesville, FL, USA, and Yun He and Zichen Shao at the Fudan University for technique support of competent cell, cell culture, and plasmid production. This work was sponsored by grants from the National Key Research and Development Program of China, grant no. 2018YFA0109400 (to C.L. and B.Z.), and the National Natural Science Foundation of China, grant no. 81972713 (to C.L.).

AUTHOR CONTRIBUTIONS

Q.Z., T.W., G.C., G.R., and Y.X. performed *in vitro* experiments. Q.Z., C.Z., and X.T. assessed, measured, and quantified the results of *in vivo* experiments. C.L. and L.Z. designed experiments. C.L., X.Z., and B.Z. analyzed the data and wrote the manuscript.

DECLARATION OF INTERESTS

The authors declare no competing interests.

REFERENCES

- Maldonado, R.F., Sá-Correia, I., and Valvano, M.A. (2016). Lipopolysaccharide modification in Gram-negative bacteria during chronic infection. *FEMS Microbiol. Rev.* *40*, 480–493.
- Beveridge, T.J. (1999). Structures of gram-negative cell walls and their derived membrane vesicles. *J. Bacteriol.* *181*, 4725–4733.
- West, A.P., Koblansky, A.A., and Ghosh, S. (2006). Recognition and signaling by toll-like receptors. *Annu. Rev. Cell Dev. Biol.* *22*, 409–437.
- Akira, S., and Takeda, K. (2004). Toll-like receptor signalling. *Nat. Rev. Immunol.* *4*, 499–511.
- Covert, M.W., Leung, T.H., Gaston, J.E., and Baltimore, D. (2005). Achieving stability of lipopolysaccharide-induced NF- κ B activation. *Science* *309*, 1854–1857.
- Kawai, T., and Akira, S. (2007). Signaling to NF- κ B by Toll-like receptors. *Trends Mol. Med.* *13*, 460–469.
- Magalhães, P.O., Lopes, A.M., Mazzola, P.G., Rangel-Yagui, C., Penna, T.C.V., and Pessoa, A., Jr. (2007). Methods of endotoxin removal from biological preparations: a review. *J. Pharm. Pharm. Sci.* *10*, 388–404.
- Wang, D., Tai, P.W.L., and Gao, G. (2019). Adeno-associated virus vector as a platform for gene therapy delivery. *Nat. Rev. Drug Discov.* *18*, 358–378.
- Li, C., and Samulski, R.J. (2020). Engineering adeno-associated virus vectors for gene therapy. *Nat. Rev. Genet.* *21*, 255–272.
- Shirley, J.L., de Jong, Y.P., Terhorst, C., and Herzog, R.W. (2020). Immune Responses to Viral Gene Therapy Vectors. *Mol. Ther.* *28*, 709–722.
- Shin, J.-H., Yue, Y., and Duan, D. (2012). Recombinant adeno-associated viral vector production and purification. *Methods Mol. Biol.* *798*, 267–284.
- Penaud-Budloo, M., François, A., Clément, N., and Ayuso, E. (2018). Pharmacology of Recombinant Adeno-associated Virus Production. *Mol. Ther. Methods Clin. Dev.* *8*, 166–180.
- Kondratova, L., Kondratov, O., Ragheb, R., and Zolotukhin, S. (2019). Removal of Endotoxin from rAAV Samples Using a Simple Detergent-Based Protocol. *Mol. Ther. Methods Clin. Dev.* *15*, 112–119.
- Miyamoto, T., Okano, S., and Kasai, N. (2009). Inactivation of *Escherichia coli* endotoxin by soft hydrothermal processing. *Appl. Environ. Microbiol.* *75*, 5058–5063.
- Piehler, M., Roeder, R., Blessing, S., and Reich, J. (2020). Comparison of LAL and rFC Assays-Participation in a Proficiency Test Program between 2014 and 2019. *Microorganisms* *8*, 418.
- Ran, G., Chen, X., Xie, Y., Zheng, Q., Xie, J., Yu, C., Pittman, N., Qi, S., Yu, F.X., Agbandje-McKenna, M., et al. (2020). Site-Directed Mutagenesis Improves the Transduction Efficiency of Capsid Library-Derived Recombinant AAV Vectors. *Mol. Ther. Methods Clin. Dev.* *17*, 545–555.
- Park, B.S., Song, D.H., Kim, H.M., Choi, B.S., Lee, H., and Lee, J.O. (2009). The structural basis of lipopolysaccharide recognition by the TLR4-MD-2 complex. *Nature* *458*, 1191–1195.
- Tarassishin, L., Suh, H.S., and Lee, S.C. (2014). LPS and IL-1 differentially activate mouse and human astrocytes: role of CD14. *Glia* *62*, 999–1013.
- Manandhar, B., Kim, H.J., and Rhyu, D.Y. (2020). *Caulerpa okamurae* extract attenuates inflammatory interaction, regulates glucose metabolism and increases insulin sensitivity in 3T3-L1 adipocytes and RAW 264.7 macrophages. *J. Integr. Med.* *18*, 253–264.
- Kumar, S., Maurya, V.K., Nayak, D., Khurana, A., Manchanda, R.K., Gadugu, S., Bhatt, M.L.B., and Saxena, S.K. (2020). *Calcarea carbonica* treatment rescues lipopolysaccharide-induced inflammatory response in human mononuclear cells via downregulation of inducible cyclooxygenase pathway. *J. Integr. Med.* *18*, 441–449.
- Reichel, F.F., Dautlebekov, D.L., Klein, R., Peters, T., Ochakovski, G.A., Seitz, I.P., Wilhelm, B., Ueffing, M., Biel, M., Wissinger, B., et al.; RD-CURE Consortium (2017). AAV8 Can Induce Innate and Adaptive Immune Response in the Primate Eye. *Mol. Ther.* *25*, 2648–2660.
- Man, S.M., Karki, R., and Kanneganti, T.D. (2017). Molecular mechanisms and functions of pyroptosis, inflammatory caspases and inflammasomes in infectious diseases. *Immunol. Rev.* *277*, 61–75.
- Rathinam, V.A.K., Zhao, Y., and Shao, F. (2019). Innate immunity to intracellular LPS. *Nat. Immunol.* *20*, 527–533.
- Hösel, M., Broxtermann, M., Janicki, H., Esser, K., Arzberger, S., Hartmann, P., Gillen, S., Kleeff, J., Stabenow, D., Odenthal, M., et al. (2012). Toll-like receptor 2-mediated innate immune response in human nonparenchymal liver cells toward adeno-associated viral vectors. *Hepatology* *55*, 287–297.
- Ran, G., Tan, D., Zhao, J., Fan, F., Zhang, Q., Wu, X., Fan, P., Fang, X., and Lu, X. (2019). Functionalized polyhydroxyalkanoate nano-beads as a stable biocatalyst for cost-effective production of the rare sugar d-allulose. *Bioresour. Technol.* *289*, 121673.
- Bong, J.H., Kim, J., Lee, G.Y., Park, J.H., Kim, T.H., Kang, M.J., and Pyun, J.C. (2019). Fluorescence immunoassay of *E. coli* using anti-lipopolysaccharide antibodies isolated from human serum. *Biosens. Bioelectron.* *126*, 518–528.
- Masarapu, H., Patel, B.K., Charoui, P.L., Hu, H., Gulati, N.M., Carpenter, B.L., Ghiladi, R.A., Shukla, S., and Steinmetz, N.F. (2017). *Physalis Mottle Virus-Like Particles* as Nanocarriers for Imaging Reagents and Drugs. *Biomacromolecules* *18*, 4141–4153.
- Watkins, H.C., Rappazzo, C.G., Higgins, J.S., Sun, X., Brock, N., Chau, A., Misra, A., Cannizzo, J.P.B., King, M.R., Maines, T.R., et al. (2017). Safe Recombinant Outer Membrane Vesicles that Display M2e Elicit Heterologous Influenza Protection. *Mol. Ther.* *25*, 989–1002.
- Gutsmann, T., Howe, J., Zähringer, U., Garidel, P., Schromm, A.B., Koch, M.H.J., Fujimoto, Y., Fukase, K., Moriyon, I., Martínez-de-Tejada, G., and Brandenburg, K. (2010). Structural prerequisites for endotoxic activity in the Limulus test as compared to cytokine production in mononuclear cells. *Innate Immunity* *16*, 39–47.
- Tan, N.S., Ng, M.L., Yau, Y.H., Chong, P.K., Ho, B., and Ding, J.L. (2000). Definition of endotoxin binding sites in horseshoe crab factor C recombinant sushi proteins and neutralization of endotoxin by sushi peptides. *FASEB J.* *14*, 1801–1813.
- Maloney, T., Phelan, R., and Simmons, N. (2018). Saving the horseshoe crab: A synthetic alternative to horseshoe crab blood for endotoxin detection. *PLoS Biol.* *16*, e2006607.

32. Mizumura, H., Ogura, N., Aketagawa, J., Aizawa, M., Kobayashi, Y., Kawabata, S.-I., and Oda, T. (2017). Genetic engineering approach to develop next-generation reagents for endotoxin quantification. *Innate Immun.* *23*, 136–146.
33. Bartel, M.A., Weinstein, J.R., and Schaffer, D.V. (2012). Directed evolution of novel adeno-associated viruses for therapeutic gene delivery. *Gene Ther.* *19*, 694–700.
34. Ling, C., Lu, Y., Cheng, B., McGoogan, K.E., Gee, S.W., Ma, W., Li, B., Aslanidi, G.V., and Srivastava, A. (2011). High-efficiency transduction of liver cancer cells by recombinant adeno-associated virus serotype 3 vectors. *J. Vis. Exp.* (49), 2538.
35. Zhong, C., Yu, Q., Jia, W., Yu, X., Yu, D., Yang, M., Wang, L., Ling, C., and Zhu, L. (2020). Mechanism for enhanced transduction of hematopoietic cells by recombinant adeno-associated virus serotype 6 vectors. *FASEB J.* *34*, 12379–12391.
36. Zhu, L.Q., Zhang, L., Zhang, J., Chang, G.L., Liu, G., Yu, D.D., Yu, X.M., Zhao, M.S., and Ye, B. (2021). Evodiamine inhibits high-fat diet-induced colitis-associated cancer in mice through regulating the gut microbiota. *J. Integr. Med.* *19*, 56–65.